Low-resolution structure of *Drosophila* translin

Vinay Kumar *, Gagan D. Gupta

High Pressure & Synchrotron Radiation Physics Division, Bhabha Atomic Research Centre, Mumbai 400085, India

ABSTRACT

Crystals of native *Drosophila melanogaster* translin diffracted to 7 Å resolution. Reductive methylation of the protein improved crystal quality. The native and methylated proteins showed similar profiles in size-exclusion chromatography analyses but the methylated protein displayed reduced DNA-binding activity. Crystals of the methylated protein diffracted to 4.2 Å resolution at BM14 of the ESRF synchrotron. Crystals with 49% solvent content belonged to monoclinic space group $P2_1$ with eight protomers in the asymmetric unit. Only 2% of low-resolution structures with similar low percentage solvent content were found in the PDB. The crystal structure, solved by molecular replacement method, refined to R_{work} (R_{free}) of 0.24 (0.29) with excellent stereochemistry. The crystal structure clearly shows that drosophila protein exists as an octamer, and not as a decamer as expected from gel-filtration elution profiles. The similar octameric quaternary fold in translin orthologs and in translin–TRAX complexes suggests an up-down dimer as the basic structural subunit of translin-like proteins. The drosophila oligomer displays asymmetric assembly and increased radius of gyration that accounts for the observed differences between the elution profiles of human and drosophila proteins on gel-filtration columns. This study demonstrates clearly that low-resolution X-ray structure can be useful in understanding complex biological oligomers.

1. Introduction

The translin proteins, of molecular mass nearly 27 kDa, bind to single-stranded DNA (ssDNA) and RNA. Translin protein was observed to be recruited to the nucleus concomitant with the induction of double strand breaks by DNA damaging agents and to function in regulating the expression of a variety of mRNA sequences by regulating RNA translocations and localization [1–4]. Translin selectivity towards RNA or DNA is modulated by interactions with GTP and another translin-like protein known as TRAX. The interactions between translin and TRAX proteins are highly conserved in eukaryotes, for instance in human, mouse, chicken, xenopus, *Drosophila melanogaster* (drosophila) and in *Schizosaccharomyces pombe* (*S. pombe*). The translin–TRAX complex binds to both ssDNA and RNA, and has recently been suggested to regulate dendritic trafficking of BDNF RNAs [5,6] as well as function as a key activator of siRNA-mediated silencing in drosophila [7]. These proteins are suggested to play a central role in eukaryotic cell biology [8,9].

Two basic nucleic acid binding motifs (basic-1 and basic-2) have been identified from the mutational studies on human and mouse translin [10,11]. The DNA-binding domain of human translin was suggested to be formed by the combination of its basic

regions in the multimeric structure, and the loss of multimeric structure resulted in abrogation of translin DNA-binding abilities [10]. Likewise, a DNA-binding incompetent P168S mutant of drosophila translin exists as a tetramer, both in solution and in crystals [12]. Currently, crystal structures of human and mouse translin proteins, which share more than 98% sequence identity [13,14] and that of drosophila P168S mutant translin [12] are known. The crystal structures of translin–TRAX heteromeric complexes of human and drosophila have also been resolved recently [15,16]. Intriguingly, biologically active translin or translin–TRAX complexes exist as octameric barrels as observed in the crystal structures analyses.

The drosophila protein has been suggested to have role in neuronal development and behavior analogous to that of mouse translin [17]. The two basic motifs considered critical for nucleic acid binding activity are not strictly conserved in drosophila translin protein that consists of 235 amino acids and shares nearly 48% sequence identity with human translin. The wild-type drosophila translin was earlier observed to correspond to octamer or decamer in the gel-filtration analysis [12]. The chicken translin was also suggested from gel-filtration and electron microscopy analyses to be a decamer with a molecular mass of about 270 kDa and an average diameter of about 94 Å [10].

The molecular dimensions, oligomeric status and protein–protein interactions in the complex biological macromolecules can be accurately determined by even a low resolution X-ray

* Corresponding author. Fax: +91 22 25505151.
  E-mail address: vinay@barc.gov.in (V. Kumar).

diffraction analysis, which can thus play important role in understanding large biological assemblies at atomic level. However, growth of well-ordered crystals of large macromolecular complexes is often a limiting factor; diffraction often is weak, anisotropic and has an effective resolution of worse than 4 Å [18]. The use of specific information from known homologous structures resolved at high resolution, however, can permit detailed structural analysis even for crystals diffracting to low-resolution [18]. The structures derived from low-resolution diffraction data are often accurate for deducing biological processes [19].

We report here crystal structure of the drosophila translin protein. The diffraction quality of the crystals could be obtained after reductive methylation of lysine residues, which diffracted to the resolution of 4.2 Å. The low-resolution data was sufficient to resolve the structure of drosophila translin, which interestingly exhibited octameric status. The native and methylated proteins showed similar profiles in size-exclusion chromatography analyses. The methylated protein also showed DNA-binding activity *albeit* with reduced affinity.

2. Results and discussion

2.1. Protein characterization

The drosophila translin protein was purified from *Escherichia coli* BL21(DE3) cells harboring *p*ET28-*dtranslin* construct by the three-step chromatographic procedure using immobilized metal affinity, anion-exchange and gel-filtration chromatography. The peak corresponding to oligomer of 295 kDa was used for crystallization and DNA-binding analysis. The protein was successfully methylated using dimethylamino–borane and formaldehyde. The reductive methylation generated high degree of modification of lysine residues. It was apparent from the MALDI–TOF analysis that all the 14 drosophila lysyl residues could be alkylated, since the molecular masses of native and methylated drosophila proteins differed by 421 Da.

The methylated drosophila protein behaved analogously to the native protein on gel-filtration column. The molecular masses of the translin oligomers were determined based on their elution profile on the molecular sieve Superdex^{TM} 200 10/300 GL column. The molecular mass of wild-type and methylated drosophila translin was estimated to be 295 kDa, as compared to molecular mass of 236 kDa determined for native human translin. Interestingly, the elution profile of human translin complexed with the 24-mer ssDNA probe also corresponded to 236 kDa. While the human translin protein exists as an octamer, the mobility on the molecular sieve column suggested that drosophila proteins could form stable octamer/decamer in solution.

2.2. Protein crystallization

An exhaustive search for diffraction-quality crystals of the native drosophila protein was not successful. However, crystals diffracting to about 4.2 Å were obtained for the methylated drosophila translin suggesting that the diffraction quality was improved by reductive methylation. The crystals of the methylated protein belonged to space group $P2_1$ with unit cell parameters $a = 91.05$ Å, $b = 131.20$ Å, $c = 96.40$ Å, $\beta = 98.46°$. Based on the experimentally determined molecular mass of the protein (29 445 Da determined by MALDI–TOF for the protein including the N-terminal poly-histidine tag and methylated lysines) and the volume of the asymmetric unit, a Matthews parameter [20] of 2.42 Å^3/Da and a solvent content of 49.1% suggested the highest normalized probability for eight protomers in the asymmetric unit [21]. The low-resolution diffraction quality of the crystals was thus

surprising as it is generally believed that protein crystals with less solvent tend to diffract better [21].

The weak diffraction of the drosophila crystals prompted us to analyze the experimental X-ray structures of the proteins alone in the Protein Data Bank (77 870 PDB entries resolved with diffraction data of resolution worse than 3.0 Å resolution using synchrotron data at 80–120 K, December 2011). The PDB structures were separated into two groups discriminated based on highest resolution of the diffraction data; group-I contained 1377 proteins resolved between 3.0 and 3.495 Å, and group-II contained 320 structures solved using data worse than 3.5 Å. The frequency distribution for the solvent content of protein crystal forms in the two groups is given in Fig. 1. The two distributions have mean values of 59.9 and 65.4, medians of 59.8 and 65.8 and modes of 57.5 and 67.5, respectively. The two data sets conform to the trend observed earlier that discriminated the structures mainly in high resolution shells; crystals diffracting to higher resolution have lower solvent content (or vice versa) [21]. Since our crystals with nearly 49% solvent content diffracted to maximum resolution of 4.2 Å, we asked how frequently the tightly packed crystals diffract to low-resolution only. We found that only 2% of the low-resolution
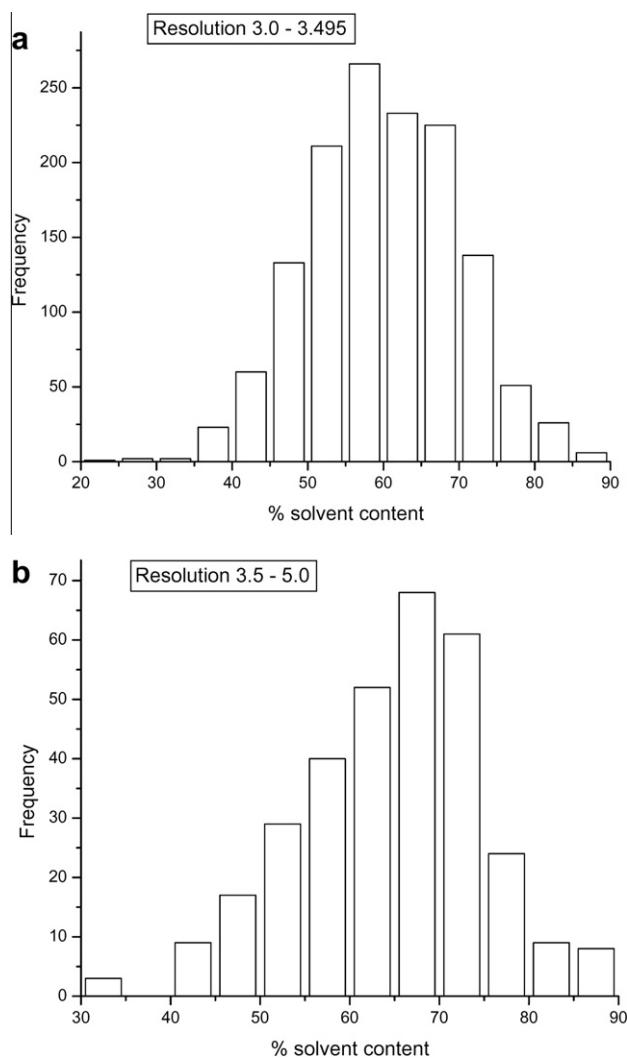

Fig. 1. Frequency distribution of percentage solvent content for non-redundant PDB structures which have been solved at 3.0 Å or worse resolution using synchrotron data collected at low temperatures (80–120 K). (A) Frequency distribution of 1377 structures solved between 3 and 3.495 Å resolution. (B) Frequency distribution of 320 structures resolved with data worse than 3.5 Å resolution.

(resolution worse than 4.0 Å) protein structures studied at sub-zero temperatures (80–120 K) using synchrotron data showed solvent content in the range 47.5–52.5%.

2.3. Crystallographic analysis

Compared to majority of low-resolution structures, the low solvent content of drosophila translin crystals resulted in highly unfavorable ratio of observations to parameters. However, low-resolution X-ray diffraction data contained sufficient information to determine reliably the structure of drosophila translin protein.

The crystal structure was solved by the molecular replacement method which identified all the eight expected translin protomers in the asymmetric unit. The initial molecular replacement phases were accurate to show electron density for the residues not included in the list of the atomic coordinates of the high resolution search model (the drosophila translin protomer obtained from the coordinates of translin–TRAX complex resolved at 2.1 Å resolution, PDB ID: 3AXJ). We also used partial structure of drosophila mutant translin (PDB ID: 2QRX; [12]) as a search model in the molecular replacement calculations. The molecular replacement search with partial structure having atomic coordinates for residues 3–187 yielded cor-
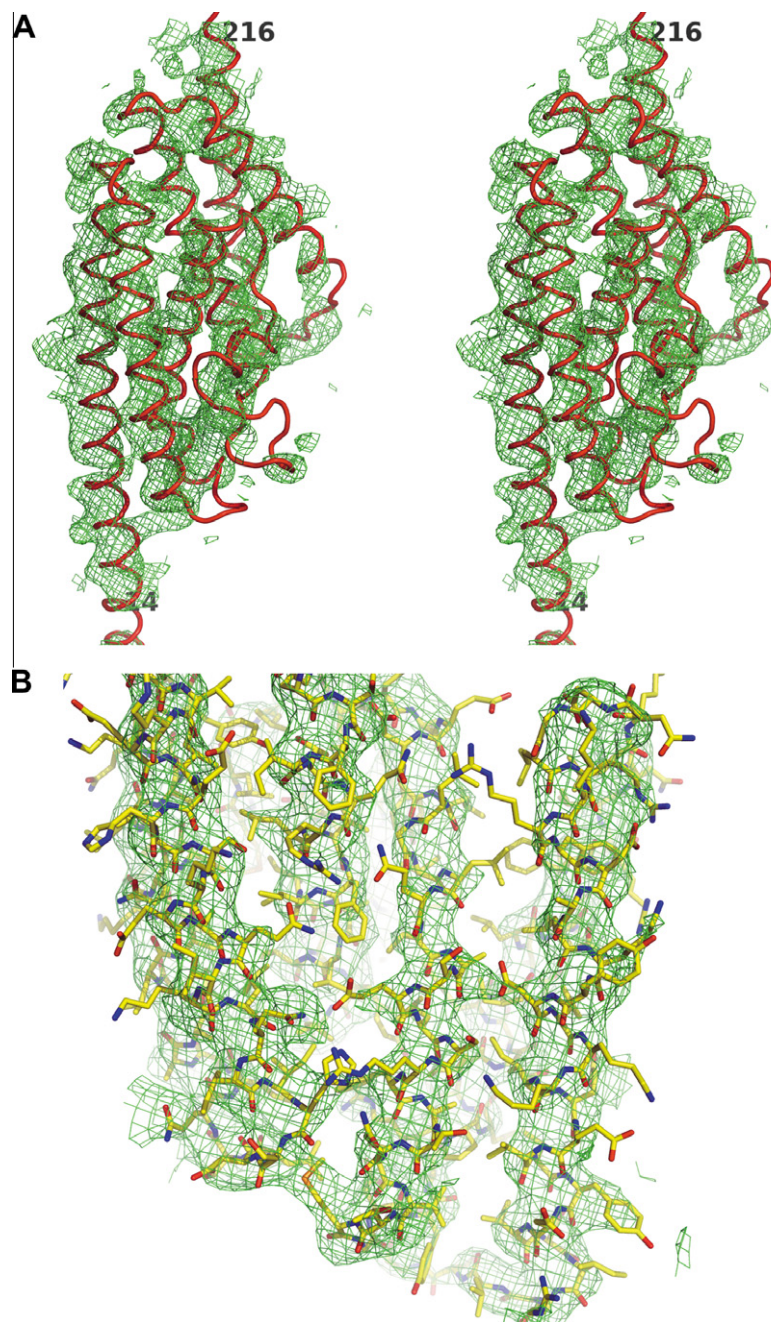
Fig. 2. (A) Stereo-view of the σA-weighted 2Fo–2Fc 'omit' electron density map (green contours) computed using Fc and phases from the rigid body refined partial structure of six protomers resolved by the molecular replacement using 2QRX as search model. The Cα trace of the seventh monomer in the refined structure (in red) is superimposed. The positions of 14th (N-terminus) and 216th (C-terminus) residues are marked. The contour level for the electron density was set to 0.7σ. (B) A section of σA-weighted 2Fo–2Fc 'filled' electron density map (green contours at 1.0σ) superposed on the refined structure. The electron density for the 'bulkier' aromatic side chains was apparent at 0.7σ contour levels. Also, traces of electron density were visible for side chains of a few smaller amino acids. The figure was prepared using PyMol software (DeLanoScientific, San Carlos, CA).

Table 1
Crystallographic data and refinement statistics.

Data statistics	
Unit cell	a = 91.05 A, b = 131.20 A, c = 96.40 Å, β=98.46°
Space group	$P2_1$
Solvent content (%)[a]	49.1
Resolution limit (Å)	4.2
Unique reflections	16416
Redundancy	3.8
Completeness (%)	99.3
R_{merge}	0.132
Mean I/mean $\sigma(I)$	5.6
Refinement statistics	
Resolution range (Å)	48–4.2
Final R_{work}/R_{free}	0.24/0.29
Number of non-hydrogen atoms	13 931
Average thermal parameter (Å^2)	184
Ramachandran plot[b]	92.5/6.1/1.4
Anisotropy (mean/sigma)[c]	0.722/0.094
Root-mean-square deviation from ideality	
Bond lengths (Å)	0.01
Bond angles (°)	1.28
Dihedral (°)	16.9

[a] As estimated from the Matthews parameter corresponding to eight protomers in the asymmetric unit.
[b] Percentages of residues in most favoured/allowed/disallowed regions of the Ramachandran plot.
[c] Results of TLS model validation using parvati server (http://skuld.bmsc.washington.edu/parvati).

rect position and orientation of six protomers. Interestingly, electron density for the other two protomers in the asymmetric unit and for the C-terminus 188–220 residues could be observed with phases from the partial model of six protomers (Fig. 2A). The electron density maps thus confirmed presence of eight protomers in the asymmetric unit and good quality of initial phases. The atomic model of eight protomers could be refined without any difficulty. The R_{work} and R_{free} after rigid-body refinement of individual protomer were 0.38 and 0.39, respectively. Different refinement protocols for improvement of precision in atomic parameters were subsequently tried. The R_{work}/R_{free} values for the models refined with different protocols were similar. The best model with minimum number of rotamer outliers was obtained with refinement of individual positional parameters, TLS groups, NCS information and bulk solvent correction (Flat bulk solvent model). The final model consisted of residues 7–220 for each of the eight protomers. Electron density was well defined for these residues and connectivity for the main-chain backbone atoms was clear at 1σ contour level in the σA-weighted 2Fo–2Fc electron density maps. The atomic coordinates for the other N-terminal (including poly-histidine tag residues) and 14 C-terminal residues are not included in the refined model, as these could not be identified in the electron density maps. The electron density for side-chain atoms was also not clearly defined, owing to which side-chain modeling in the electron density maps was difficult. It has recently been observed that application of a negative B_{sharp} value results in increased detail for side-chain conformations [18]. In order to use maps of maximum quality, different maximum-likelihood (σA) weighted maps with bulk-solvent correction and anisotropic scaling were compared. These maps were, default Phenix 'filled' maps with calculated structure factors (Fc) substituting for missing observed structure factors (Fo), maps with application of negative B_{sharp} (-50 Å^2), and average 'kicked' maps [22]. The quality of average 'kicked' maps with negative B_{sharp}, in terms of electron density for side-chain atoms, was found to be as good as default Phenix maps (Fig. 2B). The side-chain conformation

in the refined drosophila structure were thus from the high resolution model used in the molecular replacement calculations and refined by Phenix against observed structure factor amplitudes for drosophila crystals.

The refined structural model of drosophila translin protein has an R_{work} (R_{free}) of 0.24 (0.29) against all the observed data with F/$\sigma(F) \geqslant 0$ (Table 1). The evaluation using MOLPROBITY [23] revealed good stereochemistry of the structure, with nearly 93% residues in the most favored region and only 1.4% residues in the disallowed regions of the Ramachandran plot (Table 1). Further, TLS modeling was validated using the parvati server (http://skuld.bmsc.washington.edu/parvati) and it was found to be correct, except for 36 C–N linkages with CCuij < 0.950 (these had CCuij values between 0.92 and 0.95). Clearly the refinement of the model had converged to 'true' structure, as quality of the Ramachandran plot of the model, refined without secondary structure restraints, is high and as R-values (R_{work}/R_{free}) are very reasonable even with the use of NCS information during refinement steps. It was earlier noticed that low conventional R-factor cannot be achieved with a conservative NCS model at low resolution if the model is wrong [24].

2.4. Structure analysis

The oligomer of drosophila translin exists as an octamer in the crystal structure. The eight protomers in the asymmetric unit of drosophila translin crystals form an enclosed octameric barrel that is hollow inside. The structure of each of the drosophila translin protomer is comprised of seven helices (α1–α7; nomenclature as per human translin structure) and its fold is identical to that of human translin. In contrast, drosophila P168S mutant translin protomer was comprised of six helices (α1–α6) and its 47 C-terminal residues were disordered [12]. The minor differences in the structures of human and drosophila protomers are localized in the N- and C-termini residues and the loops connecting helix pairs α1/α2, α2/α3, α4/α5 and α6/α7. The two structures match with the rms deviation of 1.1 Å for 202 equivalent Cα atoms. The two protomers of translin interact in up-down conformation and form a stable dimer (Fig. 3). Nearly 2840 Å^2 (~13%) of the solvent accessible area is buried at the up-down interface on dimer formation in drosophila translin. The protein interfaces, surfaces and assemblies (PISA) service at EBI [25] estimated a gain of nearly –17.8 kcal/M in solvation free energy on the formation of the up-down dimers. The four up-down dimers of the drosophila protein superpose on each other with an rms deviation of nearly 0.95 Å and their conformations resemble the up-down dimers of human protein (Fig. 3). Nearly 424 of the 434 residues align in the structures superposed by DALI [26] with an rms deviation of 1.5 Å (Dali-iLite Z-score 26.4). Majority of the contact residues (defined as those within 3.5 Å from each other) at the up-down interface are conserved in translin orthologs, including chicken (*Gallus gallus*) translin (Fig. 4). It is possible that the functional chicken translin may also exist in the form of an octamer like its orthologs. The chicken protein shares nearly 86% sequence identity with human translin.

The up-down dimers of drosophila protein align side-by-side to form an octameric barrel of the translin molecule (Fig. 5). Importantly, the octameric quaternary fold of drosophila translin resembles human and mouse translins (PDB ID: 1J1J & 1KEY) as well as heteromeric translin–TRAX complexes of drosophila and human proteins (PDB ID: 3PJA & 3RIU). The side-by-side alignment of four up-down dimers in drosophila protein differs marginally from the human protein, which results in asymmetric assembly and larger molecular size of the drosophila protein (Fig. 6A and B).

An asymmetric assembly has recently been observed in the heteromeric complex of human translin and TRAX proteins, and was
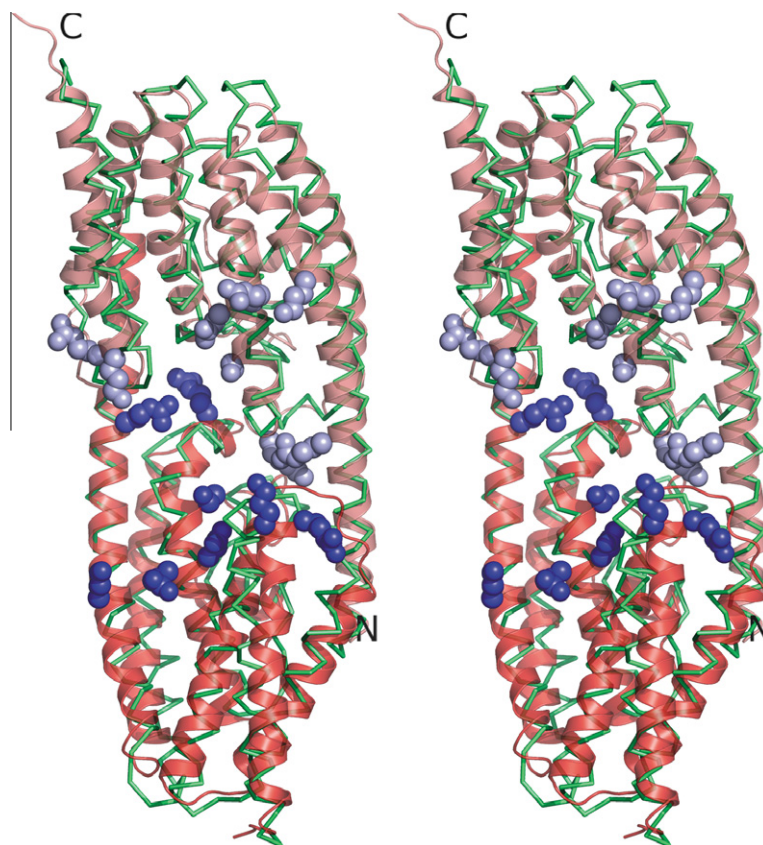
Fig. 3. Cartoon of drosophila translin up-down dimer. The two protomers of the up-down dimer are shown in the shades of red. Superposed onto the structure of drosophila translin dimer is the ribbon of human translin dimer (green). The amino and carboxy termini of one of the drosophila monomer are marked as N and C, respectively. The position of equivalent amino acid residues known to be critical for DNA-binding activity in *S. pombe* translin is represented with spheres. The substitutions of these residues of *S. pombe* translin resulted in more than 100-fold decrease in DNA-binding ability [28].

thought to be critical for the RNase activity of the complex [15]. The heteromeric translin–TRAX complex is constituted by translin–TRAX heterodimers and translin–translin homodimers. The reason for asymmetric spatial arrangement of homomeric up-down dimers in drosophila translin is not clear. Small differences in side-by-side alignment of mouse translin up-down dimers, compared to human translin, were also seen earlier [14]. Further, crystal structure of a stable form of drosophila translin–TRAX hexamer has recently been resolved [16]. The structure resembles 3/4th of the translin oligomer with one up-down dimer missing from the octameric barrel. Taken together, the available structures conform to earlier suggestion [12] that up-down dimer is the evolutionary and basic structural subunit of translin-like proteins.

The crystal structure of drosophila translin oligomer accounts for its observed behavior on size-exclusion chromatography column confirming octameric status of the protein in solution also. The radius of gyration (R_g) of drosophila and human translin octamers were computed from the atomic coordinates with Hydropro suite [27] using atomic shell model and solvent radius of 2.84 Å. The R_g of drosophila translin octamer was estimated to be 38.9 Å, compared to the value of 37.1 Å for human translin oligomer. The increased radius of gyration of drosophila protein could result in nearly 15% enhancement in its hydrodynamic volume, compared to human ortholog. This accounts for the observed differences in the elution profiles on gel-filtration column; the elution peak of the His-tagged drosophila translin corresponded to 295 kDa (molecular mass estimated from amino acid sequence, 233 kDa) compared to adjudged molecular mass of 236 kDa analyzed from

elution profile of His-tagged human translin (estimated molecular mass, 220 kDa).

2.5. DNA-binding activity

The DNA-binding activity of the drosophila translin proteins was checked for with a 24-mer Bcl–CL1 ssDNA in a gel-shift assay and was compared with the DNA-binding activity of the purified human translin under identical conditions of assay. Both the wild-type human and drosophila translin proteins showed DNA-binding activity as observed earlier [12]. Intriguingly, the methylated drosophila translin showed distinct but weaker DNA-binding activity, as adjudged from band intensities of ethidium bromide stained agarose gel (Fig. 7). The weaker binding of the methylated protein could be due to modification of Lys-194 residue which resides in the DNA-binding motif of drosophila translin ([Fig. 4]; Gupta & Kumar, unpublished results). The substitution of the equivalent Arg-211 of *S. pombe* translin caused more than 100-fold increase in the apparent K_d values for ssDNA binding [28]. While reduced activity of the chemically modified drosophila translin provides an evidence for the involvement of Lys-194 residue in binding the probe DNA, the detection of measureable activity suggests that multiple protein side chains are involved in binding the nucleic acid.

A putative nucleic acid interaction surface constituted by polar and positively charged amino acids has recently been identified in *S. pombe* translin [28]. Many of these residues were earlier identified from mutational analyses of human and mouse translins
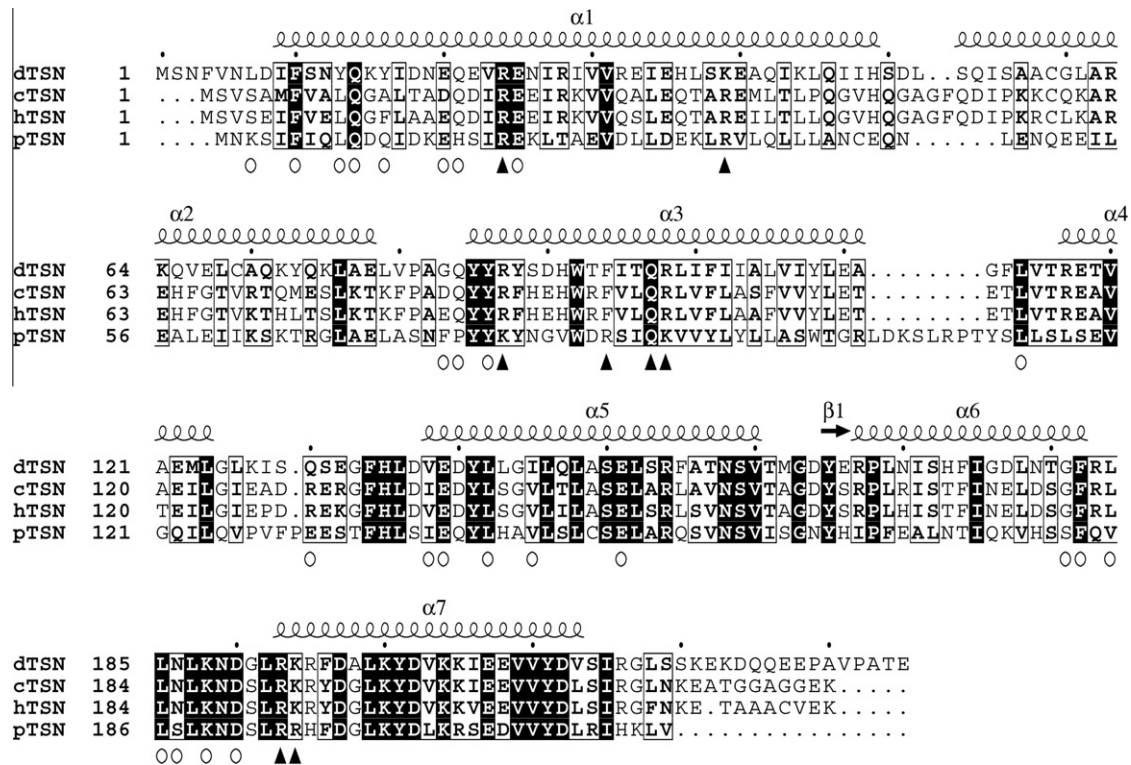
Fig. 4. Multiple sequence alignment of translin orthologs. The alignment of human translin (hTSN, UniProtKB Q15631), chicken translin (cTSN, UniProtKB P79769), drosophila translin ((dTSN, UniProtKB Q7JVK6) and *S. pombe* translin (pTSN, UniProtKB Q9P7V3) was done using PROMALS3D [38]. The identical residues are highlighted and conservative substitutions are boxed. The residues critical for ssDNA-binding activity are marked with filled triangles and residues at the up-down interface are marked with open circles. Also shown are the helices (α1–α7) for drosophila translin sequence. The figure was prepared using ESPript [39].

[10,11]. The corresponding residues of drosophila translin in multiple sequence alignment reside in the equatorial region on the inner hollow surface of the octameric barrel (Figs. 4 and 5). Identical disposition of DNA-binding residues is also observed in human translin oligomer for which elution profiles of both unbound and 24-mer DNA-bound were identical. The sequence-structure homology thus suggests similarity in ssDNA-binding mode of translin orthologs, and we expect that ssDNA binds inside the hollow octameric barrel without altering its hydrodynamic volume. In contrast, elution peak of human translin–TRAX octamer complexed with siRNA indicated higher molecular mass of the complex, compared with uncomplexed translin–TRAX heteromer [15]. This is not surprising as translin residues of basic-1 motif (86–RFHEH–90), the substitutions of which led to abrogation of RNA-binding activity [10], reside on the outer surface of the octameric barrel.

The observed plasticity in the arrangement of up-down dimers in translin-like proteins support the suggestion of Tian et al. [16] that nucleic acid can bind in the internal hollow cavity of the octameric barrel on opening of the octameric scaffold by partial dissociation. The up-down dimers are held together by less stable side-by-side interactions [12] and can dissociate from the octameric barrel structure. A detailed 3D structure of translin-nucleic acid complex should help resolving the important question of translin biology.

In conclusion, the data presented here constitute a significant advancement to the understanding of the mechanisms by which domains of translin-like proteins assemble into a biologically active complex. The low-resolution X-ray diffraction data acquired from the methylated drosophila protein crystals showed clearly that ssDNA-binding competent drosophila protein is an octamer, both in solution and in crystals. The quaternary octameric fold of drosophila translin resembles the biologically active human and mouse translin proteins and oligomers of heteromeric translin–

TRAX complexes. The strict conservation of structural domains suggests that octameric fold is constituted by four up-down dimers of translin-like proteins and is the biological active form of translin proteins. Database: structural data are available in the Protein Data Bank database PDB ID:4DG7.

3. Materials and methods

3.1. Materials

dNTPs were obtained from Roche, Germany, and restriction enzymes from New England BioLabs and *pfuTurbo* DNA polymerase was obtained from Stratagene. *E. coli* BL21(DE3) [*E. coli* B F⁻ *dcm ompT hsdS* (r_B^-, m_B^-) *galλ* (DE3)], and *p*ET28a were from Novagen. Chromatography media and pre-packed columns were obtained from Amersham-Pharmacia and Bio-Rad. Oligonucleotides for cloning and ssDNA of Bcl–CL1 sequence were synthesized at BRIT, India. Dimethylamino–borane and formaldehyde were obtained from Sigma, crystallization kits were obtained from Sigma and Hampton Research, and other fine chemicals were procured from SRL, India.

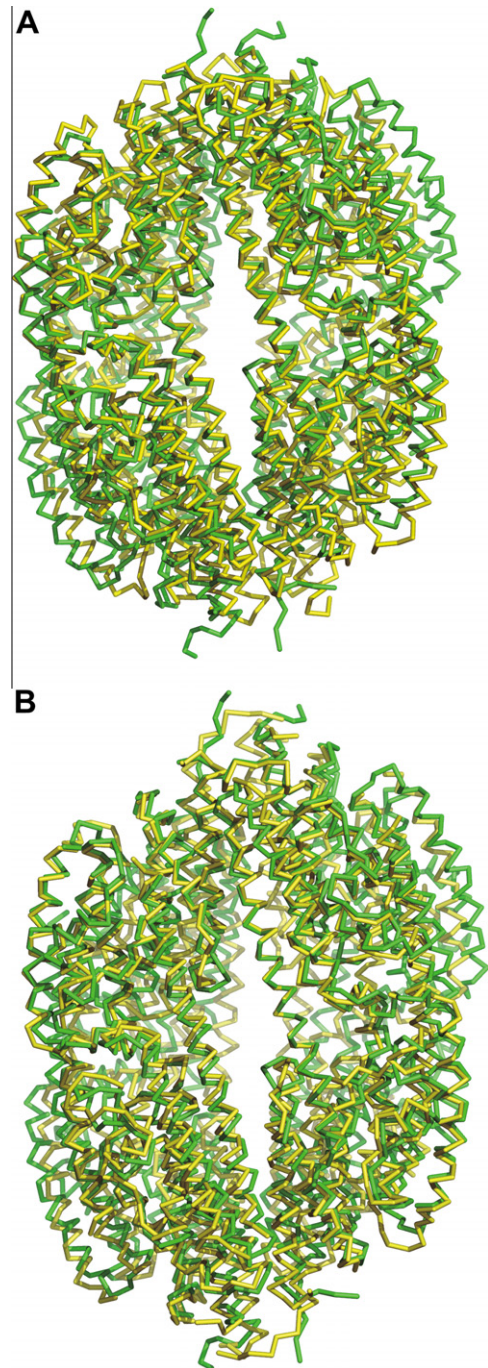### 3.2. Cloning, expression and purification of the drosophila translin

The drosophila *translin* open reading frame (ORF) was PCR amplified with *PfuTurbo* DNA polymerase using primer pair (CATCACGGACATATGTCGAACTTCGTGAACTT and ACTGGATCCTTATTCGGTTGCAGGAACAGC) and *p*QE30-*dtranslin* [12] as template. The PCR amplified product was subcloned into *Nde*I/*Bam*HI sites of *p*ET28a expression vector to express the drosophila translin protein with N-terminal poly-histidine tag (*p*ET28a-*dtranslin* construct). The construct was transformed into *E. coli*
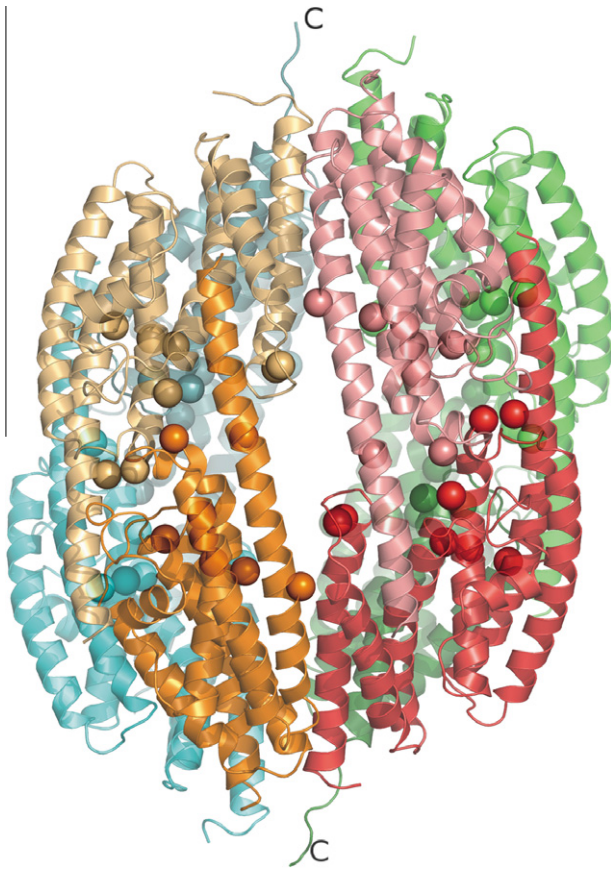
Fig. 5. Cartoon of drosophila translin octamer (at 40% transparency) composed of four up-down dimers. The protomers of the up-down down dimers are shown in similar color shades. The position of residues critical for ssDNA-binding activity is marked as spheres.

Fig. 6. The trace of polypeptide backbone of the drosophila translin octamer (green) superposed onto (A) octamer of human translin (yellow) and (B) oligomer of human translin–TRAX complex (yellow). The structural superposition was achieved using DALI [26]. The asymmetric assembly observed in translin–TRAX is also seen in drosophila oligomer.

BL21(DE3) cells for expression. The nucleotide sequence of drosophila *translin* in the construct was confirmed by complete sequencing of *translin* ORF using an automated DNA sequencer. The nucleotide sequence completely matched with drosophila *translin* gene (GenBank accession no. NM_136747).

The *E. coli* BL21(DE3) cells transformed with *p*ET28a-*dtranslin* were grown in LB media at 310 K in presence of kanamycine antibiotic (50 mg/L). The expression of drosophila translin protein was induced with 0.5 mM IPTG. After 4 h of induction, cells harvested with centrifugation were suspended in lysis buffer [25 mM Tris–HCl (pH 8.0), 100 mM NaCl, 1 mM DTT, 5% Glycerol] containing lysozyme (0.3 mg/ml) and protease-inhibitor, and were maintained on ice for 1 h. The cell suspension was sonicated for 10 min on ice in pulse mode. The cell lysate, cleared of cellular debris by centrifugation at $20000 \times g$ for 1 h, was directly loaded onto immobilized metal chelating affinity matrix (Ni-IDA) equilibrated with buffer A1 [25 mM Tris–HCl (pH 8.0), 100 mM NaCl and 50 mM imidazole]. The column was extensively washed with buffer A1 and the bound proteins were eluted with a linear gradient of imidazole (50–400 mM) in buffer A1. The translin protein eluted at ~200 mM concentration of imidazole. The eluted protein was directly loaded onto pre-packed Q-sepharose column pre-equilibrated with buffer A2 [25 mM Tris–HCl (pH 8.0), 100 mM NaCl]. After extensive wash with buffer A2, the bound proteins were eluted with a linear gradient of 100–500 mM NaCl in buffer A2. The drosophila translin protein eluted at nearly 350 mM NaCl. The eluted protein fractions were treated with DNase1 and RNaseA

overnight at 293 K, and the drosophila protein was purified using Ni-IDA matrix. The purified protein was dialyzed against storage buffer [25 mM Tris–HCl (pH 8.0), 100 mM NaCl] and concentrated to 10 mg/ml using centricon (Millipore, USA). The drosophila protein was stored at 277 K. The purification progress was monitored by 12–15% SDS–PAGE. The N-terminal His-tagged human translin (encoded by *p*QE9-*tsn* construct) was purified from *E. coli* BL21 (DE3) expression system as reported earlier [29].
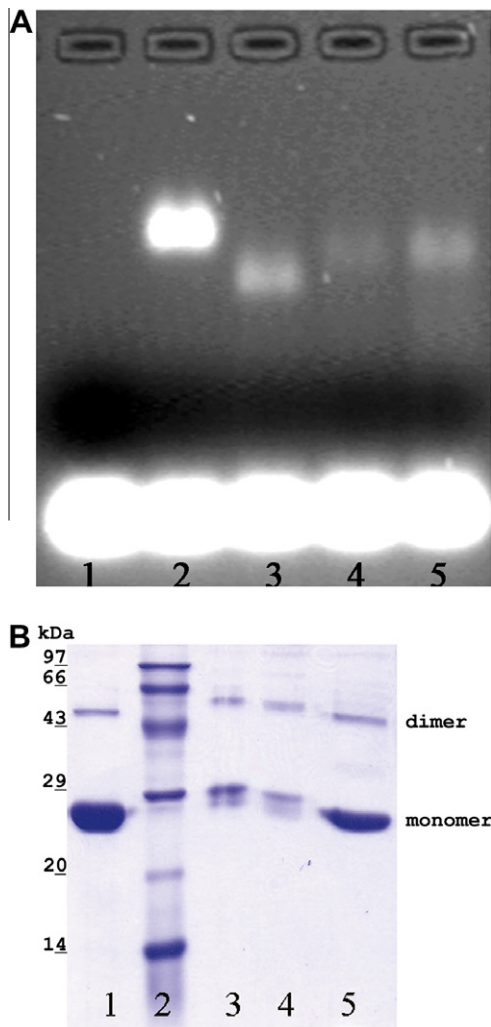
Fig. 7. Analysis of DNA-binding activity of the translin proteins. (A) Bcl–CL1 24-mer ssDNA (200 pmol) was separately incubated with the known concentrations of RNaseA and DNaseI treated translin proteins. The mixtures were analyzed on 1.5% agarose gel and stained with ethidium bromide; lane 1, only DNA; lane 2, human translin (50 pmol of octameric translin); lane 3, wild-type drosophila translin (50 pmol of octameric translin); lanes 4 and 5 for methylated drosophila translin (50 and 100 pmol of the octameric protein, respectively). (B) Analysis of the gel-shifted complex on SDS–PAGE. Translin gel shifted complex obtained with ssDNA was excised from the corresponding lanes of stained agarose gel and the gel-pieces loaded onto the SDS–PAGE gel and subjected to electrophoresis; lanes 1, purified human translin; lane 2, standard molecular-weight markers (masses given on the left); lanes 3, 4 and 5, gel-retarded bands of lanes 5 (methylated drosophila translin), 3 (wild-type drosophila translin) and 2 (human translin), respectively. Bands corresponding to dimers were also observed for purified translin (lane 1) as well as for the gel-retarded bands (lanes 3–5).

3.3. Reductive methylation

The methylation experiment was based on the protocol described by Shaw et al. [30]. The protein was transferred to buffer D [50 mM HEPES (pH 8.0), 200 mM NaCl] by centrifugation buffer exchange using centricon tubes with a 10 kDa molecular-weight cutoff. It was concentrated to 10 mg/ml. For each 1 ml of protein solution in 1.5 ml eppendorf tube, 20 μL of 1 M dimethylamine–borane complex (DMAB) solution was added followed by addition of 40 μL of 1 M formaldehyde solution. The eppendorf tube was maintained at 277 K and was continuously shaken. The addition of DMAB and formaldehyde was repeated twice after every 2 h. Subsequently, 60 μL of DMAB was added to the reaction mixture and was incubated for 18 h at 277 K. The reaction was terminated

by the addition of Tris–HCl (pH 8.0) to the final concentration of 100 mM. Dimethylamino–borane and formaldehyde were removed from the protein by buffer exchange against buffer [25 mM Tris–HCl (pH 8.0), 25 mM NaCl], using 50 ml pre-packed column of P-6 matrix. The methylation was verified via MALDI–TOF mass spectrometry.

3.4. Gel-filtration and DNA-binding assay

The wild-type human and drosophila translins, methylated drosophila translin and human translin–DNA (24-mer probe) complex, were loaded on the Superdex™ 200 10/300 GL column for final purification step as well as for molecular-weight determination. The Superdex™ 200 column was calibrated with gel-filtration molecular-weight markers (Amersham-Pharmacia; carbonic anhydrase, 29 kDa; alcohol dehydrogenase, 150 kDa; β-amylase, 200 kDa; ferritin, 440 kDa). The major eluted peak of each independent gel-filtration experiment was adjudged on SDS–PAGE. The DNA-binding status of human translin–DNA complex elution peak was confirmed by ratio of UV absorption at 260 and 280 nm. The purified proteins were concentrated to 10 mg/ml. The protein concentrations were estimated by modified Lowry's method [31] using bovine serum albumin as the standard.

Electrophoresis mobility shift assays (EMSA) were performed to assess DNA-binding activity of the DNase1 and RNaseA treated proteins using Bcl–CL1 ssDNA (GCCCTCCTGCCCTCCTTCCGCGGG) as probe. The molecular masses of the drosophila proteins used were nearly 295 kDa and that of human translin was 236 kDa. Translin proteins (50 or 100 pmol of the octameric proteins) were incubated with the DNA probe (200 pmol) in 20 μL of reaction volume in binding buffer B1 [25 mM Tris–HCl (pH 8.0), 100 mM NaCl, 1 mM EDTA] for 30 min. The products were resolved by electrophoresis on 1.5% agarose gel and stained with ethidium bromide. The agarose regions containing gel-shifted bands were excised and adjudged on 12% SDS–PAGE.

3.5. Crystallization of the protein and data collection statistics

Crystallization of the wild-type and methylated drosophila translin proteins was attempted using CyBi®-CrystalCreator robotics and a number of formulated crystallization screens viz., basic and extended Sigma crystallization kits, and salt-RX, PEG-grid and low-ionic screens from Hampton Research. The wild-type protein yielded crystals with a number of conditions containing PEG-6000 (16–20%) or with ammonium sulfate (1–2 M). However, despite exhaustive search none of these crystals of sizes $100 \times 100 \times 200$ μm^3 diffracted to better than 7–8 Å resolution. Also, a large number of crystallization trials showed protein aggregation in the drops. The use of non-detergent sulphobetaines (NDSB-256) to improve the crystal quality did not solve the problem.

Diffraction-quality crystals of the methylated protein were obtained by sitting-drop method using Intelli-Plate 48-2 (ARI, Hampton) crystallization plates and PACT++ crystallization conditions. The initial hits were optimized during which sodium format was observed to promote crystal growth rapidly. The crystals of the methylated protein of the size about $70 \times 70 \times 80$ μm^3 were obtained using 20% PEG-4000, 100 mM bicine (pH 8.5), 200 mM sodium formate and 5% glycerol. The crystallization condition itself contained reasonable concentration of cryoprotectant and these were found to be optimum using X-rays from a laboratory source. These crystals belonged to space group $P2_1$ and diffracted to about 4.2 Å resolution using synchrotron X-rays under cryo-conditions. The 3-dimensional diffraction intensity data for the crystals of the methylated protein were acquired on a CCD detector with 1.0° oscillation per image at the beam-line BM14-U of the Euro-

pean Synchrotron Radiation Facility (ESRF). The data were processed using HKL-2000 [32]. The data statistics is summarized in Table 1.

3.6. Structure solution and refinement

The initial phases for the methylated drosophila translin crystals were obtained by the molecular replacement method using the program Phenix [33] and atomic coordinates of the monomer of the drosophila translin taken from the high resolution structure of translin–TRAX complex (PDB ID: 3AXJ) and partial structure of the drosophila P168S mutant translin listing atomic coordinates for residues 3–187 (PDB ID: 2QRX; [12]) as search models. The use of atomic coordinates corresponding to residues 1–213 of drosophila translin protomer (PDB ID: 3AXJ) revealed eight protomers of drosophila translin in the asymmetric unit. However, molecular replacement search using atomic coordinates for residues 3–187 of the mutant drosophila protein could locate only six copies correctly in the asymmetric unit. The initial phases with both the molecular replacement solutions were reasonably accurate such that electron density for the 7–220 residues of eight protomers could be identified into the electron density maps. The eight protomers were individually refined as rigid body using Phenix. The individual coordinates were subsequently refined by Phenix with maximum-likelihood target and with a little model building using COOT [34]. The manual corrections of the model were restricted to fitting of the polypeptide segments, and not the side-chain conformation of individual amino acids, against the σA corrected Fourier maps [35]. Refinement of the model was monitored by R_{work} and R_{free} [36]. Several refinement schemes suggested for structure improvement against low resolution data [18,19,37] were tried during the cycles of refinement with Phenix viz., refinement of the individual atomic positional parameters (XYZ refinement) with or without TLS (translation/libration/screw) groups, TLS refinement with torsion angle molecular dynamics, or XYZ refinement with TLS and secondary structure restraints. Non-crystallographic symmetry (NCS) information and bulk solvent correction were applied in all the trials, and each protomer was treated as an independent TLS group.

3.7. Analysis of PDB data

From the PDB containing nearly 77 870 structure coordinate entries (December 2011), experimental X-ray structures of the proteins alone determined to resolution worse than 3.0 Å resolution using synchrotron data at 80–120 K were downloaded. To reduce the possibility of statistical bias and create non-redundant sets, homologues with 90% sequence identity were clustered. The non-redundant PDB structures were further separated into two groups based on highest resolution of the diffraction data; group-I contained 1377 proteins resolved between 3.0 and 3.495 Å, and group-II contained 320 structures solved using data worse than 3.5 Å. The Matthews parameter (V_M) and percentage solvent content reported in structure coordinate entries were extracted from the coordinate files and their frequency were analyzed in the two resolution groups. Descriptive statistics (limits, mean, median, and mode) were calculated for the frequency distributions of V_M and solvent content.

References

[1] Kwon, K.Y. and Hecht, N.B. (1993) Binding of a phosphoprotein to the 3′ untranslated region of the mouse protamine 2 mRNA temporally represses its translation. Mol. Cell. Biol. 13, 6547–6557.

[2] Han, J.R., Yiu, G.K. and Hecht, N.B. (1995) Testis/brain RNA-binding protein attaches translationally repressed and transported mRNAs to microtubules. Proc. Natl. Acad. Sci. USA 92, 9550–9554.

[3] Aoki, K., Suzuki, K., Sugano, T., Tasaka, T., Nakahara, K., Kuge, O., Omori, A. and Kasai, M. (1995) A novel gene Translin, encodes a recombination hotspot binding protein associated with chromosomal translocations. Nat. Genet. 10, 167–174.

[4] Kasai, M., Matsuzaki, T., Katayanagi, K., Omori, A., Maziarz, R.T., Strominger, J.L., Aoki, K. and Suzuki, K. (1997) The Translin ring specifically recognizes DNA ends at recombination hot spots in the human genome. J. Biol. Chem. 272, 11402–11407.

[5] Li, Z., Wu, Y. and Baraban, J.M. (2008) The Translin/Trax RNA binding complex: clues to function in the nervous system. Biochim. Biophys. Acta 1779, 479–485.

[6] Chiaruttini, C., Vicario, A., Li, Z., Baj, G., Braiuca, P., Wu, Y., Lee, F.S., Gardossi, L., Baraban, J.M. and Tongiorgi, E. (2009) Dendritic trafficking of BDNF mRNA is mediated by translin and blocked by the G196A (Val66Met) mutation. Proc. Natl. Acad. Sci. USA 106, 16481–16486.

[7] Liu, Y., Ye, X., Jiang, F., Liang, C., Chen, D., Peng, J., Kinch, L.N., Grishin, N.V. and Liu, Q. (2009) C3PO, an endoribonuclease that promotes RNAi by facilitating RISC activation. Science 325, 750–753.

[8] Jaendling, A. and McFarlane, R.J. (2010) Biological roles of translin and translin-associated factor-X: RNA metabolism comes to the fore. Biochem. J. 429, 225–234.

[9] Lluis, M., Hoe, W., Schleit, J. and Robertus, J. (2010) Analysis of nucleic acid binding by a recombinant translin–trax complex. Biochem. Biophys. Res. Commun. 396, 709–713.

[10] Aoki, K., Suzuki, K., Ishida, R. and Kasai, M. (1999) The DNA binding activity of translin is mediated by a basic region in the ring-shaped structure conserved in evolution. FEBS Lett. 443, 363–366.

[11] Chennathukuzhi, V.M., Kurihara, Y., Bray, J.D., Yang, J. and Hecht, N.B. (2001) Altering the GTP binding site of the DNA/RNA-binding protein, Translin/TB-RBP, decreases RNA binding and may create a dominant negative phenotype. Nucleic Acids Res. 29, 4433–4440.

[12] Gupta, G.D., Makde, R.D., Roa, B.J. and Kumar, V. (2008) Crystal structures of *drosophila* mutant translin and characterization of translin variants reveal the structural plasticity of translin proteins. FEBS J. 275, 4235–4249.

[13] Sugiura, I., Sasaki, C., Hasegawa, T., Kohno, T., Sugio, S., Moriyama, H., Kasai, M. and Matsuzaki, T. (2004) Structure of human translin at 2.2 Å resolution. Acta Cystallogr. D60, 674–679.

[14] Pascal, J.M., Hart, P.J., Hecht, N.B. and Robertus, J.D. (2002) Crystal structure of TB-RBP, a novel RNA-binding and regulating protein. J. Mol. Biol. 319, 1049–1057.

[15] Ye, X., Huang, N., Liu, Y., Paroo, Z., Huerta, C., Li, P., Chen, S., Liu, Q. and Zhang, H. (2011) Structure of C3PO and mechanism of human RISC activation. Nat. Struct. Mol. Biol. 18, 650–657.

[16] Tian, Y., Simanshu, D.K., Ascano, M., Diaz-Avalos, R., Park, A.Y., Juranek, S.A., Rice, W.J., Yin, Q., Robinson, C.V., Tuschl, T. and Patel, D.J. (2011) Multimeric assembly and biochemical characterization of the TRAX–translin endonuclease complex. Nat. Struct. Mol. Biol. 18, 658–664.

[17] Suseendranathan, K., Sengupta, K., Rikhy, R., D'Souza, J.S., Kokkanti, M., Kulkarni, M.G., Kamdar, R., Changede, R., Sinha, R., Subramanian, L., Singh, K., Rodrigues, V. and Rao, B.J. (2007) Expression pattern of Drosophila translin and behavioral analyses of the mutant. Eur. J. Cell Biol. 86, 173–186.

[18] Brunger, A.T., DeLaBarre, B., Davies, J.M. and Weis, W.I. (2009) X-ray structure determination at low resolution. Acta Crystallogr. D 65, 128–133.

[19] Schröder, G.F., Levitt, M. and Brunger, A.T. (2010) Super-resolution biomolecular crystallography with low-resolution data. Nature 464, 1218–1222.

[20] Matthews, B.W. (1968) Solvent content of protein crystals. J. Mol. Biol. 33, 491–497.

[21] Kantardjieff, K.A. and Rupp, B. (2003) Matthews coefficient probabilities: improved estimates for unit cell contents of proteins, DNA, and protein–nucleic acid complex crystals. Protein Sci. 12, 1865–1871.

[22] Praaenikar, J., Afonine, P.V., Guncar, G., Adams, P.D. and Turk, D. (2009) Averaged kick maps: less noise, more signal and probably less bias. Acta Crystallogr. D 65, 921–931.

[23] Chen, V.B., Arendall 3rd, W.B., Headd, J.J., Keedy, D.A., Immormino, R.M., Kapral, G.J., Murray, L.W., Richardson, J.S. and Richardson, D.C. (2010) MolProbity: all-atom structure validation for macromolecular crystallography. Acta Crystallogr. D 66, 12–21.

[24] Kleywegt, G.J. (1996) Use of non-crystallographic symmetry in protein structure refinement. Acta Crystallogr. D 52, 842–857.

[25] Krissinel, E. and Henrick, K. (2007) Inference of macromolecular assemblies from crystalline state. J. Mol. Biol. 372, 774–797.

[26] Holm, L. and Rosenström, P. (2010) Dali server: conservation mapping in 3D. Nucleic Acids Res. 38, W545–W549.

[27] Ortega, A., Amoros, D. and Garcia de la Torre, J. (2011) Prediction of hydrodynamic and other solution properties of rigid proteins from atomic- and residue-level models. Biophys. J. 101, 892–898.

[28] Eliahoo, E., Ben, Y.R., Pérez-Cano, L., Fernández-Recio, J., Glaser, F. and Manor, H. (2010) Mapping of interaction sites of the *Schizosaccharomyces pombe* protein Translin with nucleic acids and proteins: a combined molecular genetics and bioinformatics study. Nucleic Acids Res. 38, 2975–2989.

[29] Gupta, G.D., Makde, R.D., Kamdar, R.P., D'Souza, J.S., Kulkarni, M.G., Kumar, V. and Rao, B.J. (2005) Co-expressed recombinant human Translin–Trax complex binds DNA. FEBS Lett. 579, 3141–3146.

[30] Shaw, N., Cheng, C. and Liu, Z.-J (2007) Procedure for reductive methylation of protein to improve crystallizability. http://dx.doi.org./doi:10.1038/nprot.2007.287.

[31] Miller, G.L. (1959) Protein determination for large number of samples. Anal. Chem. 31, 964.

[32] Otwinowski, Z. and Minor, W. (1997) in: Processing of X-ray Diffraction Data Collected in Oscillation Mode, Methods in Enzymology (Carter, C.W. and Sweet, R.M., Eds.), 276, pp. 307–326, Academic Press, NY.

[33] Adams, P.D., Afonine, P.V., Grosse-Kunstleve, R.W., Read, R.J., Richardson, J.S., Richardson, D.C. and Terwilliger, T.C. (2009) Recent developments in phasing and structure refinement for macromolecular crystallography. Curr. Opin. Struct. Biol. 19, 566–572.

[34] Emsley, P. and Cowtan, K. (2004) Coot: model-building tools for molecular graphics. Acta Crystallogr. D 60, 2126–2132.

[35] Read, R.J. (1986) Improved Fourier coefficients for maps using phases from partial structure with errors. Acta Crystallogr. A 42, 140–149.

[36] Brunger, A.T. (1997) Free R value: cross validation in crystallography. Methods Enzymol. 277, 366–396.

[37] Merritt, E.A. (2011) TLS and all that. CCP4 summer school.

[38] Pei, J., Kim, B.H. and Grishin, N.V. (2008) PROMALS3D: a tool for multiple protein sequence and structure alignments. Nucleic Acids Res. 36, 2295–2300.

[39] Gouet, P., Robert, X. and Courcelle, E. (2003) ESPript/ENDscript: extracting and rendering sequence and 3D information from atomic structures of proteins. Nucleic Acids Res. 31, 3320–3323.